MATRIX TECHNIQUE AND ITS APPLICATION IN THE FIELD OF CHEMICAL PHYSICS

G. C. Pimentel

Chemistry Department, University of California, Berkeley, California, U.S.A.

INTRODUCTION

During the last decade, the matrix isolation technique has been developed rapidly and fruitfully. Electronic spectroscopy, infra-red spectroscopy and electron spin resonance methods have been employed. Any one of these detection methods could provide the entire subject of this paper: to do justice to all three would be difficult. The following review of some current applications of the matrix technique is confined to studies based on infra-red spectroscopy.

The matrix isolation method involves the spectroscopic detection of a molecular species dispersed in a spectroscopically distinct host matrix, either a crystal or a glass. The purposes are to obtain a particular set of controlled environmental conditions and/or accumulation of a suitable amount of an otherwise inaccessible species. The matrix materials can be divided into three classes—ionic crystals, inert gas crystals, and molecular solids. Each of these classes has its own special capabilities. An ionic crystal acts as an isolating matrix when it forms a very dilute solid solution. The solute ion is thus placed, presumably, in an ordered, ionic environment which is reasonably well understood. The inert gases also may provide a nicely ordered lattice environment, but with much weaker forces and complete absence of chemical reactivity. The variety of molecular solids which can be used provides a spectrum of environments bridging these two extremes.

PREPARATION OF MATRIX SAMPLES

Most, but not all, of the ionic crystal studies have employed alkali halide host lattices. Solid solutions in alkali halides can be prepared by cooling a molten solution, by precipitation from aqueous solution, by vaporization and condensation, by freeze-drying, or by diffusion. Diffusion can be brought about by heating a mixture of two ionic solids, by grinding two ionic solids against each other, and, most conveniently, by use of the pressed disc technique. There are obvious precautions needed in the pressed disc method: the amount of solute must not exceed the solubility or the spectrum of the matrix-isolated sample will be obscured by the spectrum of the pure solid. Also, the time of pressing the disc should be ample (a half-hour or more at high pressure is usually needed) to ensure uniformity of the distribution.

A hydrocarbon glass can be used as a matrix and it is readily formed by rapid cooling of the liquid. The rapid rise of viscosity is presumed to prevent

aggregation of the solute. Such samples are quite transparent to visible light, a considerable advantage.

The other common mode of preparing matrix samples is through rapid freezing of a gas mixture. Such a sample is generally highly scattering. Furthermore, diffusion and aggregation can readily occur unless the temperature is kept well below half the melting point at all times during deposition. To reduce both scattering and diffusion, the rate of deposition must be extremely slow. A typical rate would be in the range 25–200 μmoles/min. The deposit time is sometimes as long as 10 h since the spectroscopic study may require between 10 and 100 μmoles of solute at a matrix/solute mole ratio as high as a few thousand.

The gas mixture is usually prepared by standard vacuum line procedures. A technique with interesting possibilities is to trap species diffusing out of an oven (e.g. a King furnace) or a Knudsen cell. The reactive species must then be mixed with a stream of matrix gas and transported to the window without opportunity for reaction.

ILLUSTRATIVE EXAMPLES OF APPLICATIONS

So much work has accumulated, particularly over the last three or four years, that a comprehensive review would become fragmentary. Instead the discussion will be restricted to a number of examples sufficient to illustrate potentialities and unsolved problems.

Detection of reactive molecular species

There is a long list of free radicals which have been detected in matrix studies through electron spin resonance, thanks to the extreme sensitivity of the detection method. Porter and co-workers have detected perhaps twenty-five complex-free radicals trapped in organic glasses using electronic spectroscopy in the visible and near ultra-violet[1]. Robinson has detected some ten more[2]. By comparison, the list of reactive molecular species detected by infra-red methods is much shorter. Nitroxyl[3], HNO, and formyl[4], HCO, have been detected in the Berkeley laboratories. Isomeric forms of N_2O_4 and N_2O_3 have been described on the basis of matrix work by Fateley, Bent, and Crawford[5]. Monomeric lithium fluoride, LiF, has been isolated in inert gas matrices by Linevsky[6]. Van Thiel and Pimentel described a hydrogen bonded complex $H_3N \cdot HN_3$ in solid nitrogen demonstrating that the stability of the ionic form, $NH_4^+N_3^-$ depends upon the crystal lattice. The hydride ion, H^-, will be reported here at this meeting by Price, Sherman, Smart, and Wilkinson[7].

Though this list is short, it is perhaps as significant as the much longer lists mentioned earlier. Formyl radical, HCO, offers probably the first definite detection of any free radical with three or more atoms by any infra-red method except for NO_2. The detection of the isomeric form of N_2O_4 may lead to a clarification of the chemistry of nitrogen dioxide. The study of monomeric LiF can be confidently expected to stimulate a large volume of similar work. The species H^- has not, to my knowledge, been definitely identified earlier by any spectroscopic method at all.

Reactions of free radicals

Because of its general applicability, the infra-red region provides a conven-ient method for studying reactions of free radicals under matrix conditions. The unique interest of such work derives from the isolation of the reactants in the inert cage and the resultant interruption of chemistry shortly after the primary reaction. The free radical is produced by photolysis of a suitable parent molecule *in situ* in an inert matrix containing a small amount of a desired reactant. Some of the reactions which have been so studied are shown in *Table 1*.

Table 1. Reactions of free radicals studied under matrix conditions

Reaction			Reference
H	+ CO	→ HCO	4
$O(^1D)$	+ N_2	→ N_2O	8
$O(^1D)$	+ N_2O	→ 2NO	8
$O(^3P)$	+ CO	→ CO_2	9
$O(^3P)$	+ C_2H_2	→ H_2CCO	9, 10
NH	+ O_2	→ HONO	11
CH_3	+ CH_3CD_3	→ CH_4, CH_3D	12

The type of information which results can be shown by examples. In the reaction of $O(^3P)$ atoms with CO, an upper limit is placed on the activation energy for this reaction (8·1 kcal/mole)[9]. No other value of ΔH† has been reported; indeed, there was no earlier proof that ^3P oxygen atoms react with CO. The reaction of $O(^3P)$ and acetylene to form ketene was discovered for the first time[10]. The ratio of CH_4 to CH_3D obtained from the reaction of CH_3 (from photolysis of CH_3I) with CD_3CH_3 provides information on the cage effect[12]. Though the energy of the methyl radical (~ 32 kcal/mole) is rapidly degraded, the ratio of CH_4 to CH_3D is that expected for gaseous CH_3 radicals at a thermodynamic temperature near 2,000 °K.

Spectral peculiarities

The matrix spectra offer a considerable challenge and great interest to the spectroscopist. The spectral features are usually sharp, so that frequency accuracy can be high. Sharp spectra permit detailed analyses of frequency shifts, band widths, intensities, and other esoteric matters close to the hearts of spectroscopists. It is already clear that valuable information on inter-molecular forces will result. Three examples of studies which have recently appeared in the literature will show the directions of interpretation which are being explored. The examples show, also, that clarification has not yet been reached.

Maki and Decius[13] have studied solid solutions of cyanate ion, NCO^-, in four alkali halide lattices: KI, KBr, KCl, and NaCl. *Figure 1* reproduces some of their spectra. As the temperature is lowered, the spectrum reveals a wealth of detail and bands sufficiently well defined to permit frequency accuracy of $\pm 0·3$ cm^{-1}. Convincing identification was made for one

or more absorptions due to each of the isotopic species $^{14}N^{12}C^{16}O$, $^{14}N^{12}C^{18}O$, $^{15}N^{12}C^{16}O$, $^{14}N^{13}C^{16}O$, $^{14}N^{13}C^{18}O$, and $^{15}N^{13}C^{16}O$ at the natural abundances. Detailed normal co-ordinate analysis was possible, extending even to the determination of anharmonicity constants and the splittings of Fermi doublets. Maki and Decius are able to make the substantial claim that "the agreement is, on the whole, not inferior to that reported for the gaseous molecules CO_2 and N_2O".
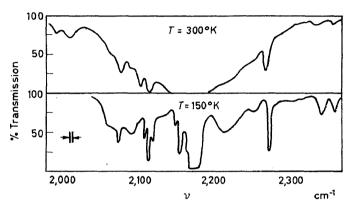

Figure 1. A portion of the infra-red spectrum of cyanate ion in KBr[13]

These workers continue the analysis of their data by seeking an understanding of the frequency changes caused by the various matrix materials. They attempt to determine the long-range forces by evaluating the induction energy (sometimes called the reaction field) caused by dipole-induced dipole interactions of a dipole embedded in a uniform polarizable medium. The simple Kirkwood–Bauer–Magat treatment is improved by a direct summation of the interactions between a single (point) dipolar solute molecule and the entire lattice of polarizable alkali and halide ions. Equation (1):

$$V'_{ab} = - [\mu_a^2 \alpha_b (3 \cos^2 \theta_a + 1)]/2r^6 \qquad (1)$$

(where V'_{ab} is the dipole-polarizability interaction energy, μ_a is the dipole moment of solute molecule a, α_b is the polarizability of lattice ion b, θ_a is the angle between the dipole axis of a and the line connecting a and b, and r is the distance between a and b), is summed over the lattice to give the term shown in the third column of *Table 5*. In this expression there is no ambiguity about the value to be given to the distance parameter, r; it is exactly the alkali halide unit cell dimension. From an estimate of the dipole derivative, the results shown in *Table 2* are obtained for ω_3, the asymmetric stretching frequency of NCO^-.

Observing that the calculated shifts are small and trend in the wrong direction, Maki and Decius[13] conclude that "although the induction energy exerts a . . . measurable influence on the frequencies, the repulsive (short range) interactions must also be considered". They treat these repulsive interactions only qualitatively.

Table 2. Frequency shifts for ω_3 of NCO⁻ due to dipole-induced dipole interaction (after Maki and Decius[13])

Matrix	$\Delta\omega$ *(calc.)* (cm^{-1})	ω_3 (cm^{-1})
KI	−4·6	2,155·8
KBr	−5·3	2,169·6
KCl	−6·0	2.181·8
NaCl	−7·4	2,211·2

Ketelaar and co-workers have carried out extensive studies of this sort[14−16]. Of the ione studied, NO_3^-, NO_2^-, HF_2^-, BF_4^-, BH_4^- and NH_4^+, the bifluoride ion shows the most striking behaviour. All of these ions show a characteristic net of frequencies for a given mode, as influenced by the lattice.
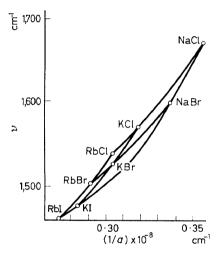

Figure 2. The ν_3 absorption frequency of bifluoride ion in various alkali halide matrices plotted v. the reciprocal of the lattice parameter.

A typical net is shown in *Figure 2.* Van der Elsken also considers the dipole-induced dipole interactions, but following more closely the Kirkwood–Bauer–Magat treatment beginning in the form:

$$v_0^2 - v^2 = \frac{2}{a^3} \times \frac{\epsilon - 1}{2\epsilon + 1} \times \frac{1}{4\pi^2}\left(\frac{\partial\mu}{\partial Q}\right)_0^2 = C\frac{n^2 - 1}{2n^2 + 1} \qquad (2)$$

where v_0 is the gas phase frequency, v is the matrix frequency, a is the cavity radius, ϵ is the solvent dielectric constant, $(\partial\mu/\partial Q)$ is the dipole derivative with respect to the normal co-ordinate Q, and n is the solvent refractive index. Since the gas phase frequency is not known, he rearranges equation (2) to the form shown in the third column of *Table 5.* The quantity C is assigned a range of values and the resulting calculations of Δv can be applied as corrections to the observed frequencies. If all of the frequency shifts can be accounted for by equation (2), then there should exist a value of C such that all of

the corrected frequencies would be identical. This is not the case, as shown in *Figure 3*. The best that can be done is to select the value of $C(C = 0.4)$ which brings all of the corrected frequencies on to a smooth curve. (The corrections[17] which do so for ν_3 of HF_2^- are of the order of 110 to 140 cm^{-1}. For comparison, these corrections are near 25 cm^{-1} for the ν_4 mode of BH_4^-.) Thus the conclusion is reached that the network character of the observed frequencies can be assigned to dipole-induced dipole interactions, but that other and larger interactions are influential. Since the smooth curve extends from 1560 cm^{-1} (HF_2^- in RbI) to 1750 cm^{-1} (HF_2^- in NaCl), the shift not yet accounted for is of the order of 190 cm^{-1}.
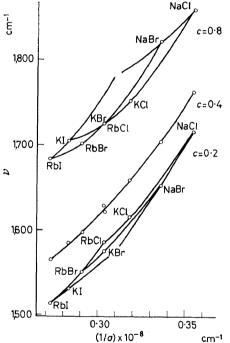

Figure 3. Application of the Kirkwood–Bauer–Magat theory to the ν_3 absorption frequency of bifluoride ion in various alkali halide matrices[16]

Van der Elsken analyses several possible additional terms. Arguments are presented which suggest that short-range forces, repulsion and van der Waals attraction, are relatively unimportant in the case of HF_2^-. Firstly, the effects would be expected to concentrate in the symmetric stretching mode. Instead, the asymmetric stretching mode is most affected. Second, two alkali halide matrices, RbCl and KBr, give about the same frequency for ν_3 (respectively, 1540 and 1527) though the cavity sizes are quite different.

Van der Elsken focuses attention on electrostatic effects as the probable cause. Assuming a point charge model of HF_2^- and a particular orientation of the ion in the cubic lattice, he shows that there are two possible contributions to frequency shifts. The interaction of a point-charge model of HF_2^- with the electrostatic field adds new energy terms which contribute to the

vibrational force constants. In addition, forces are exerted on the HF_2^- molecule which alter the internuclear distances. If the potential function is anharmonic, the new equilibrium configuration will be characterized by different force constants. The argument cannot be made in an unambiguous way, and the most that can be said is that the remainder of the frequency shifts might be explainable on the basis of electrostatic interactions.

Linevsky has conducted a study which contrasts in an interesting way with the alkali halide matrix work. He suspended LiF (monomer, presumably) in inert gas and nitrogen matrix solids[6]. He, too, attempted to analyse the frequency shifts observed. In the matrices Ar, Kr, Xe, and N_2, there are no electrostatic effects. Linevsky calculates the induction effect in a manner similar to that used by Maki and Decius, summing over the lattice for an assumed perfect cubic lattice with a substitutional site occupied by the LiF molecule. Instead of expressing the result in terms of $(\partial\mu/\partial Q)_0^2$, he calculates the perturbation of the ith harmonic oscillator level by the average dipole moment of the ith state. Equation (3):

$$W_i = -\frac{\alpha\mu_i^2}{2r^6}(3\cos^2\theta + 1) \tag{3}$$

(where W_i is the energy perturbation of the ith harmonic state, μ_i is the average dipole moment of the ith state, and α, θ, and r are as defined in equation (1)), summed over the entire lattice, permits him to derive the expression of frequency shift shown in the last column of *Table 5*, and to take advantage of the known values of μ_1^2 and μ_0^2 derived from the values of $(\mu^2 I)_{v=1}$ and $(\mu^2 I)_{v=0}$ (where I is the moment of inertia) reported by Braunstein and Trischka[18]. The calculated frequency shifts are all about the same and, though large, are not large enough to explain all of the observed shifts. The results are shown in *Table 3*, the observed shifts being calculated from the gas phase frequency of LiF, $v = 900$ cm^{-1}, as reported by Vidale[18]. Linevsky assigns all of the discrepancy to dispersion interactions. This leaves a rather large dispersion effect, a term omitted in other treatments.

Table 3. Calculated and observed frequency shifts: LiF in various matrix materials at 4°K

Matrix	Observed Δv (cm^{-1})	Dipole–induced dipole Δv (cm^{-1})	Dipole–quadrapole Δv (cm^{-1})	Dispersion Δv (cm^{-1})
A	− 65	− 45	—	(− 20)
Kr	− 70	− 45	—	(− 25)
Xe	− 77	− 45	—	(− 32)
N_2	− 122	− 40	− 55	(− 27)

The nitrogen matrix shift is even larger, being −122 cm^{-1}. Linevsky attributes this to the presence of an additional interaction, the dipole–quadrapole interaction, due to the quadrapole moment of nitrogen. The expression used by Linevsky for this contribution is also shown in the last

column of *Table 5*. *Table 3* shows that the sum of the calculated dipole-induced dipole and dipole–quadrapole interactions still leaves a discrepancy of 27 cm^{-1}, about the same order of magnitude as the discrepancies assigned to dispersion forces in the inert gas matrices. The proposal that the nitrogen matrix shifts are influenced by the quadrapole moment receives some indirect support from recent matrix work in the Berkeley laboratories[20]. Frequency shifts have been measured accurately for four of the fundamental absorptions of HN$_3$ in various matrices. Some of the data are shown in *Table 4*. The

Table 4. Frequency shifts for hydrazoic acid in various matrices

Matrix	Quadrapole	$\Delta\nu = \nu_{mx} - \nu_{gas}$ (cm^{-1})			
		N—H stretching	N$_3$(a) stretching	N$_3$(s) stretching	N—N—H bending
Ar	0	− 12	− 2	− 5	− 6
N$_2$	$1\cdot49 \times 10^{-26}$	− 13	+ 8	+ 3	+ 15

positive shifts of three of the modes may be associated with the dipole-quadrapole interaction present in nitrogen matrix. Preliminary studies with other matrices with non-zero quadrapole moments are consistent (CO and CO$_2$).

Turning now to *Table 5*, we can compare the results. Firstly, the shifts calculated by Linevsky for dipole-induced dipole interactions are much larger than those calculated by Maki and Decius and smaller than those calculated by Ketelaar and van der Elsken. Though each group considers a different system, the range of the calculations seems to be too large. (It should be noted that LiF probably has an unusually large change of dipole moment with vibrational excitation. Hence smaller values than Linevsky's would be normally expected.) The magnitude of the dispersion term deduced by Linevsky gives further reason to pause. This term is quite usually neglected in considerations of the origin of solvent shifts, though conceivably it should not be. Whatever the resolution of these various calculations of matrix shifts, it seems likely that progress here will cast light on the related but less tractable problem of correlating solvent shifts in solutions.

CONCLUSION

In conclusion, it should be observed that many of the problems which can be attacked with the matrix technique are substantially aided by the coupling of different methods of study. In the detection and study of free radicals, the sensitivities of electron resonance and electronic spectroscopy offer great advantage. Infra-red spectra, on the other hand, often reveal chemical processes taking place which would be unnoticed by the other detection methods. With reference to spectral perturbations, interpretations of electronic and infra-red absorption shifts, band widths and intensities are complementary. Together, they offer a more complete view of intermolecular interactions than can be obtained from either alone.

Table 5. A contrast of calculations of frequency shifts in matrix studies

	Maki and Decius[13] NCO⁻ in MX	Ketelaar and van der Elsken[15-17] HF₂⁻ in MX	Linevsky[6] LiF in Ar, N₂
Dipole-polarization (induction, reaction field)	$\dfrac{\Delta \nu}{\nu} = \dfrac{1}{4\pi^2 c^2 \nu^2}\left(\dfrac{\partial \mu}{\partial Q}\right)_0^2 \left(\dfrac{b\alpha - + d\alpha +}{a^6}\right)$ $\sim -5\ \text{cm}^{-1}$	$\Delta \nu = \dfrac{1}{2}\nu' \pm \dfrac{1}{2}\sqrt{\nu'^2 + 4C\dfrac{n^2-1}{2n^2+1}}$ $\sim -125\ \text{cm}^{-1}$	$\Delta \nu = \dfrac{b\alpha(\mu_1^2 - \mu_0^2)}{a^6}$ $-45\ \text{cm}^{-1}$
Dispersion: polarization–polarization, van der Waals	Assumed $= 0$	Assumed $= 0$	By difference $= -25\ \text{cm}^{-1}$
Repulsions	By difference $\sim 60\ \text{cm}^{-1}$	Assumed $= 0$	Assumed $= 0$
Ion-dipole "electrostatic"	By symmetry $= 0$	Calculated $\sim 150\ \text{cm}^{-1}$	Not present
Quadrupole-dipole	Not present	Not present	$\Delta \nu = \dfrac{bQN_2(\mu_1 - \mu_0)}{a^4} = -55\ \text{cm}^{-1}$

References

[1] G. Porter and E. Stracham. *Trans. Faraday Soc.*, **54,** 1595 (1958)

[2] G. W. Robinson. *J. Mol. Spectroscopy*, **6,** 58 (1961)

[3] H. W. Brown and G. C. Pimentel. *J. Chem. Phys.*, **29,** 883 (1958)

[4] G. E. Ewing, W. E. Thompson and G. C. Pimentel. *J. Chem. Phys.*, **32,** 927 (1960)

[5] W. G. Fateley, H. A. Bent and B. Crawford. *J. Chem. Phys.*, **31,** 204 (1959)

[6] M. J. Linevsky. *J. Chem. Phys.*, **34,** 587 (1961)

[7] W. C. Price, W. F. Sherman, C. Smart and G. R. Wilkinson. 5th European Congress on Molecular Spectroscopy, Amsterdam (1961)

[8] W. B. De More. *Ph.D. Thesis*, California Institute of Technology, Pasadena, Calif. (1958)

[9] I. Haller. *Ph.D. Thesis*, University of California, Berkeley, Calif. (1961)

[10] I. Haller and G. C. Pimentel. *J. Chem. Phys.*, in press

[11] J. D. Baldeschwieler and G. C. Pimentel. *J. Chem. Phys.*, **33,** 1008 (1960)

[12] C. D. Bass and G. C. Pimentel. *J. Am. Chem. Soc.*, in press

[13] A. Maki and J. C. Decius. *J. Chem. Phys.*, **31,** 772 (1959)

[14] J. A. A. Ketelaar, C. J. H. Shutte and B. L. Schram. *Spectrochim. Acta*, **13,** 336 (1959)

[15] J. a. A. Ketelaar, C. Haas and J. van der Elsken. *J. Chem. Phys.*, **24,** 624 (1956)

[16] J. van der Elsken. *Ph.D. Thesis*, University of Amsterdam (1959)

[17] J. van der Elsken. 7th Colloq. Spectroscopicum intern., *Rev. Universelle des Mines, Ser.* **9** No. 5 (1959)

[18] R. Braunstein and J. W. Trischka. *J. Phys. Rev.*, **98,** 1092 (1955)

[19] G. Vidale. *J. Phys. Chem.*, **64,** 314 (1960)

[20] S. Charles and G. C. Pimentel. Unpublished results